Vapor-Phase Strategy to Pillaring of Two-Dimensional Zeolite

Lu Wei,[†,‡] Kechen Song,[‡,§] Wei Wu,[‡] Scott Holdren,[∥] Guanghui Zhu,[⊥] Emily Shulman,[‡] Wenjin Shang,[#] Huiyong Chen,[#] Michael R. Zachariah,[∥,±] and Dongxia Liu[*,‡]

[†]College of Materials Science and Engineering, Beijing University of Technology, Beijing 100124, P. R. China
[‡]Department of Chemical and Biomolecular Engineering, University of Maryland, College Park, Maryland 20742, United States
[§]School of Chemical and Environmental Engineering, China University of Mining and Technology, Beijing, 100083, China
[∥]Department of Chemistry and Biochemistry, University of Maryland, College Park, Maryland 20742, United States
[⊥]School of Chemical and Biomolecular Engineering, Georgia Institute of Technology, Atlanta, Georgia 30332, United States
[#]School of Chemical Engineering, Northwest University, Xi'an, Shanxi 710069, China

S *Supporting Information*

ABSTRACT: Two-dimensional (2D) layered zeolites are new forms of 3D zeolite frameworks. They can be pillared to form more open porous structures with increased access for reactants that are too big for the micropores of zeolites. The current pillaring procedure, however, requires intercalation of pillaring precursors by dispersing 2D zeolite in an alkoxide liquid and hydrolizing entrapped alkoxide to form inorganic oxide pillars in an aqueous alkaline solution. Both steps use excess solvents, generate significant waste, and require multiple synthesis and separation steps. Here we report a vapor-phase pillarization (VPP) process to produce pillared zeolites from 2D layered zeolite structures. The VPP process has ~100% efficiency of alkoxide usage in the intercalation step, requires less (and, in some cases, zero) water addition in the hydrolysis step, does not require separation for product recovery, and generates no liquid waste. Furthermore, synthesis of pillared zeolites via the VPP process can be accomplished within a single apparatus with one-time operation. The pillared zeolite prepared by the VPP method preserved the zeolitic layered structure as well as acidity and showed enhancement in catalytic alkylation of mesitylene with benzyl alcohol compared to 2D layered zeolite without pillarization treatment.

Two-dimensional (2D) layered zeolites contain a stack of microporous crystalline aluminosilicate sheets, each of which has one or a fraction of the unit-cell thickness, equivalent to a few nanometers.[1−4] The atoms within the zeolitic layers are connected by strong covalent bonds, while the contiguous zeolitic layers are linked by van der Waals forces, hydrogen bonds, or ionic interactions (i.e., interaction between terminal silanol groups and charged structure directing agents).[5−7] The interlayer interactions in 2D zeolites determine the potential for a variety of structural and chemical modifications within the interlayer space between adjacent zeolitic layers with preservation of the original layer integrity. Therefore, 2D zeolite materials can be considered as host scaffolds that can expand and/or extend via structural, topotactic, and compositional modifications to form novel and diverse structures.

Two basic chemical processes, exfoliation[8−14] and pillarization,[15−25] have been used to modify 2D zeolites into diverse structures. The exfoliation process separates the stack of 2D zeolite nanosheets into self-standing independent entities by breaking down the interlayer interactions. The exfoliated zeolite nanosheets can be used as a base material for the fabrication of membranes[26−28] or used directly as hierarchical catalysts.[29−31] Rather than breaking down the stack of 2D zeolites in the exfoliation process, the pillarization process transforms the 2D zeolites into hierarchical materials with the retention of the stacked layer structure. The pillarization often involves subsequent expansion of interlayer space by swelling with long chain polar organic molecules, intercalation of the swollen materials in an alkoxide liquid, hydrolysis of entrapped alkoxide in an aqueous alkaline solution, and removal of organics as well as transformation of alkoxide liquid into permanent oxide pillars between zeolitic layers by calcination.[16−19,22] The current pillaring procedure requires multiple discrete steps, uses excess solvents in both intercalation and hydrolysis treatments, and generates waste.

Here, we report on a vapor-phase pillarization (VPP) process to produce pillared zeolites from 2D layered zeolite materials. The experimental setup (Figure 1) is similar to that used in steam-assisted zeolite crystallization[32,33] in a Teflon-lined autoclave. A glass vial containing 2D layered zeolite is
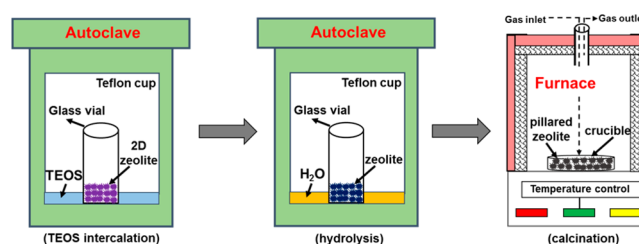

Figure 1. Schematic of the formation of pillared zeolite from 2D layered zeolite in the VPP process.

placed in the Teflon cup. The pillaring precursor (i.e., liquid alkoxide) is dropped into the Teflon cup and separated from the 2D layered zeolite by the glass container. After heating the autoclave to evaporate alkoxide for intercalation, the same setup is used to evaporate water for hydrolysis of intercalated alkoxide (Section S1). The mass ratios of alkoxide/zeolite and water/zeolite are controlled as 0.5 and 10 in the intercalation and hydrolysis steps, respectively. The 2D layered zeolite is calcined in a furnace to form the pillared zeolite. In comparison to pillarization of 2D layered zeolites in liquid solvent/solution reported previously,[16−19,22] the VPP method requires up to ~10 times less alkoxide in the intercalation step, uses less (and even zero, to be discussed below) water addition in the hydrolysis step, does not require product recovery from the liquid solvent/solution, and generates no liquid waste.

As a prominent representative of 2D layered zeolite, multilamellar MFI (M-MFI),[31] synthesized by hydrothermal crystallization of a synthetic gel comprising zeolite precursor materials and a diquanternary ammonium template (Section S1.2), was used as the precursor (M-MFI(P)) to form pillared MFI (PMFI) zeolite using the VPP process. Tetraethyl orthosilicate (TEOS) and deionized water (DI H_2O) were used in the intercalation and hydrolysis steps, respectively, to form silica (SiO_2) pillars in PMFI. Figure 2a shows the XRD
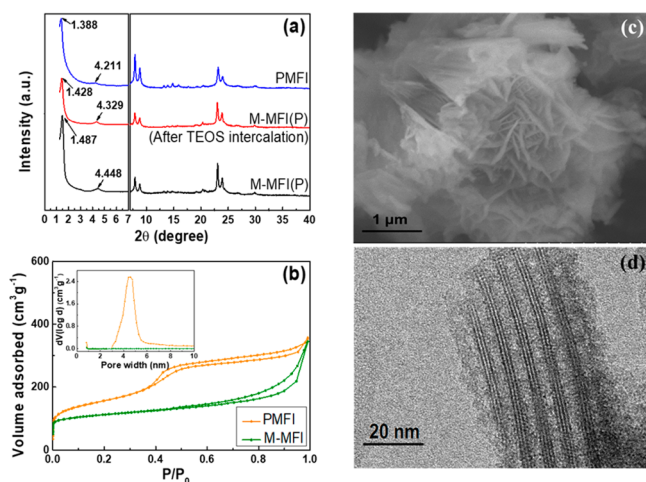

Figure 2. Characterization of PMFI formed in VPP process. (a) XRD patterns M-MFI(P) at different synthesis stages and PMFI and (b) N_2 isotherm of PMFI and M-MFI samples. (c and d) SEM and TEM images of PMFI zeolite. (VPP conditions: 0.1 g of M-MFI(P), 0.05 g of TEOS, 1 g of H_2O, intercalation at 423 K for 24 h, hydrolysis at 353 K for 24 h.)

patterns of M-MFI(P) and M-MFI(P) after TEOS intercalation and PMFI synthesized using the VPP process. The characteristic diffraction peaks of the MFI structure[31] in the wide-angle range in Figure 1a suggest that crystalline MFI framework was retained in the VPP process. The low-angle diffraction peaks[22,34] indicate preservation of the 2D layered structure in pillarization. The N_2 isotherms and pore size distributions (Figure 2b) show that PMFI has much higher surface area and mesoporosity than M-MFI prepared from direct calcination of M-MFI(P). The PMFI prepared with the VPP process preserves the nanosheet aggregate morphology of M-MFI(P)[31] (scanning electron microscopy (SEM) image in Figure 2c). The ordering of zeolitic nanosheets is clearly

visualized by transmission electron microscopy (TEM) of PMFI in Figure 2d.

To explore the influence of TEOS quantity on formation of PMFI in the VPP process, the mass ratio of TEOS to M-MFI(P) (i.e., TEOS/M-MFI(P)) was varied from 0.05 to 3.75 (Section S2.1). The bulk morphology of the M-MFI(P) sample after the intercalation step transformed from a white, dry powder into a pale yellow gel with increasing TEOS usage (Figure S1). The TEOS liquid in the Teflon cup had disappeared when the TEOS/M-MFI(P) ratio was below 0.5, while TEOS liquid droplets appeared on the walls of both the Teflon cup and glass vial with TEOS/M-MFI(P) ratios of 1.00 and 3.75. The appearance of a "bump" peak ($2\theta \sim 13.5°$) in the wide-angle XRD (Figure S2) of PMFI synthesized with a TEOS/M-MFI(P) ratio of 1.00 and 3.75 indicates the emergence of amorphous material from an excess of TEOS. The disappearance of diffraction peaks in the low-angle XRD of PMFI synthesized with a TEOS/M-MFI(P) ratio of 0.05 suggests collapse of the layered zeolitic structure since the SiO_2 pillars formed using TEOS concentrations were insufficient to maintain the layered structure integrity upon organic template removal via calcination. The TEOS/M-MFI(P) ratio of 0.50 and 0.10 produced PMFI with high crystallinity, ordering of zeolitic nanosheet layers, and high mesoporosity (isotherm data in Figure S3 and Table S1). The intercalation temperature did not influence PMFI formation significantly under investigated conditions. The XRD patterns (Figure S4) and N_2 isotherms (Figure S5) of PMFI synthesized at intercalation temperatures of 363, 383, 403, and 423 K with the VPP process are very similar.

The effects of water in the hydrolysis step on PMFI formation were examined by varying the mass ratio of water to M-MFI(P) (H_2O/M-MFI(P)) from 10 to 0 in the VPP process. In all cases, PMFI was synthesized successfully, as confirmed by both XRD (Figure S6) and N_2 isotherm (Figure S7) data. The formation of PMFI can be completed even with no water added, which is unexpected since water is considered a required material for TEOS hydrolysis to form the pillars.[35] However, since the M-MFI(P) was dried in a convective oven at 343 K for 12 h after the hydrothermal crystallization, it is likely that adsorbed water remained in the porous zeolite structures. Alkali ions and diquanternary ammonium template molecules trapped in M-MFI(P) from the hydrothermal synthesis provide sufficient basicity for TEOS hydrolysis, since a pH of 8 (by NaOH solution) is commonly used in the liquid-phase pillarization in previous methods.[16−19,22] The thermogravimetric analysis (TGA) (Figure S8) shows that M-MFI(P) contains ~16% H_2O, which closely corresponds to the water amount required for complete hydrolysis of TEOS in the intercalation step (calculation details see Section S2.3). This is consistent with the fact that the pillared structure was unable to form when the M-MFI(P) sample was dried in a vacuum oven at 393 K for 12 h (absence of low-angle XRD peaks in Figure S9).

The zero water addition in the VPP process suggests an option to further simplify the zeolite pillarization protocol. In this case, we eliminated the TEOS hydrolysis step and integrated TEOS intercalation and zeolite calcination steps into one apparatus to realize a one-time operation for the synthesis of PMFI zeolite. In the new VPP protocol, the apparatus is a furnace containing a quartz "U"-shaped tube (Figure 3, for details refer to Section S1.3). The 2D layered zeolite is added into the "bulb" region of the quartz tube from
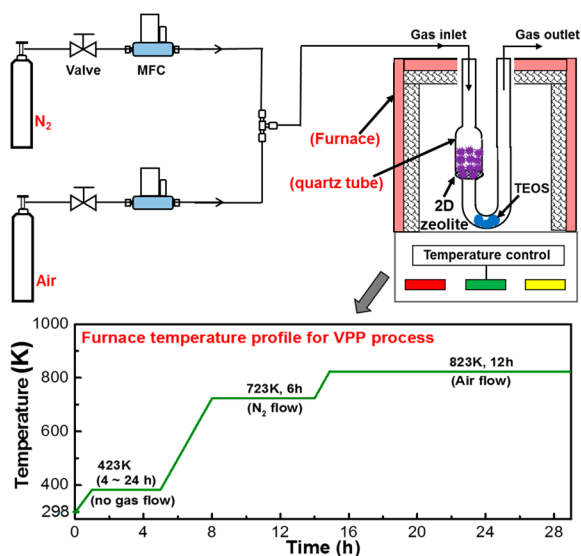
Figure 3. Experimental configuration and temperature profile for VPP of 2D zeolite in one unit under one-time operation.

Figure 4. Acidity and catalytic performance of PMFI prepared by VPP process. (a) DRIFTS spectra, (b) FTIR spectra of adsorbed pyridine, (c) ^{29}Si (top panel) and ^{27}Al (bottom panel) MAS NMR, and (d) benzyl alcohol conversion of mesitylene, respectively.

one opening, while liquid alkoxide solvent is dropped from the other opening. A quartz frit isolates the 2D layered zeolite from direct contact with alkoxide liquid before the VPP process starts. After operating the furnace according to the temperature profile shown in Figure 3, PMFI (confirmed by XRD (Figure S10) and N2 isotherm (Figure S11) in the Supporting Information) was formed along with complete TEOS consumption. Therefore, the entire VPP process only requires a single apparatus and one-time operation and does not require further separation for product recovery or generate liquid waste; this process can achieve ~100% efficiency in zeolite and TEOS utilization for the formation of pillared zeolite.

The composition, acidity, and catalytic performance of PMFI synthesized from the VPP process was characterized. The silicon (Si) and aluminum (Al) contents of PMFI are nearly identical to those calculated using M-MFI(P) and TEOS quantities, assuming all TEOS was consumed during the transformation into SiO_2 pillars (Table S2). This confirms the complete consumption of alkoxide liquid in the VPP process, which is consistent with visual observation. FTIR spectra of the OH-stretching mode ($\nu(OH)$) and adsorbed pyridine in PMFI and M-MFI (Figure 4a,b) were recorded to understand their acidity properties. In Figure 4a, three peaks centered around 3739, 3674, and 3614 cm^{-1} are associated with terminal silanol (Si–OH) groups, extra-framework Al–OH species, and Brønsted acid site (Si–O(H)–Al) groups,[36−38] respectively, on both M-MFI and PMFI. Both samples showed comparable characteristic peaks for Brønsted (1545 cm^{-1}) and Lewis (1450 cm^{-1}) acid sites[36,38,39] in the FTIR spectra of adsorbed pyridine (Figure 4b). These results indicate acidity properties of the 2D zeolites were not destroyed during the VPP process. Solid state NMR (Figure 4c) was employed to investigate the local bonding environment of Si and Al species in the PMFI zeolite by recording the ^{29}Si single pulse (SP) and ^{27}Al NMR spectra. In the top panel, the peak (−113 ppm) corresponding to the crystallographically nonequivalent Q^4 tetrahedral sites (Q^n stands for X_{4-n}Si-$[OSi]_n$)[34,40,41] is much stronger than that of Q^3 sites (−103 ppm) arising from the silanol groups. In the bottom panel, the peak at 55 ppm is due to the tetrahedrally coordinated
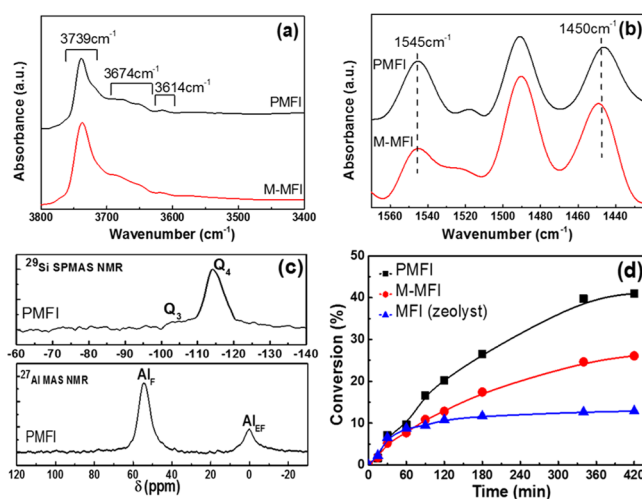
framework aluminum (Al_F), whereas the peak around 0 ppm is due to an octahedral coordination typical of extra-framework Al (Al_{EF}).[19,31] The NMR spectrum of PMFI prepared via the VPP process is similar to that of M-MFI[31] and PMFI synthesized by the liquid phase pillarization method.[34] The catalytic conversion of benzyl alcohol in mesitylene, a reaction that requires mesoporosity in MFI to enable high activity,[25,42−44] shows that PMFI had higher benzyl alcohol conversion than M-MFI and conventional MFI (Figure 4d; for experimental details, see Section S1.5), suggesting the successful formation of a pillared hierarchical zeolite structure for space-demanding catalytic reactions. The catalytic performance of PMFI prepared by the VPP process is comparable to that synthesized by the conventional liquid-phase pillarization approach (Figure S12).

In conclusion, we demonstrate that the pillarization of 2D layered zeolite can be accomplished by the VPP method that integrates three discrete operation steps (intercalation, hydrolysis, and calcination, typically practiced in zeolite pillarization) into a single operation using only one apparatus. The VPP protocol has ~100% efficiency in usage of alkoxide liquid as well as zeolite materials and does not generate liquid waste. The pillared zeolite prepared using the VPP process has preserved the structural integrity (both framework crystallinity and ordering of zeolitic nanosheet layers), acidity, and catalytic performance of the zeolite framework in comparison to 2D zeolite prepared using direct calcination. The VPP process is scalable, easy to operate, remarkably simple, and highly efficient compared to the previous liquid-phase pillarization method, which could pave a new avenue toward pillaring additional 2D zeolites and new types of layered materials.

■ ASSOCIATED CONTENT

Ⓢ Supporting Information

The Supporting Information is available free of charge on the ACS Publications website at DOI: 10.1021/jacs.9b03479.

> Experimental details for synthesis and characterization of M-MFI(P), M-MFI and PMFI; catalyst preparation for catalysis study and details in catalysis tests; additional XRD and N$_2$ isotherm and TGA analyses (PDF)

■ AUTHOR INFORMATION

Corresponding Author
*E-mail: liud@umd.edu.

ORCID ●

Wei Wu: 0000-0003-2392-6546
Huiyong Chen: 0000-0003-0045-3141
Michael R. Zachariah: 0000-0002-4115-3324
Dongxia Liu: 0000-0001-8712-2219

Present Address
±Department of Chemical and Environmental Engineering, University of California, Riverside (mrz@engr.ucr.edu).

Notes
The authors declare no competing financial interest.

■ REFERENCES

(1) Díaz, U. *Layered Materials with Catalytic Applications: Pillared and Delaminated Zeolites from MWW Precursors*; ISRN Chemical Engineering; 2012, Article ID 537164.

(2) Li, C.; Moliner, M.; Corma, A. Building Zeolites from Precrystallized Units: Nanoscale Architecture. *Angew. Chem., Int. Ed.* **2018**, *57*, 15330.

(3) Přech, J.; Pizarro, P.; Serrano, D. P.; Čejka. From 3D to 2D zeolite catalytic materials. *Chem. Soc. Rev.* **2018**, *47*, 8263.

(4) Roth, W. J.; Nachtigall, P.; Morris, R. E.; Čejka, J. Two-Dimensional Zeolites: Current Status and Perspectives. *Chem. Rev.* **2014**, *114*, 4807.

(5) Marler, B.; Gies, H. Hydrous layer silicates as precursors for zeolites obtained through topotactic condensation: a review. *Eur. J. Mineral.* **2012**, *24*, 405.

(6) Roth, W. J.; Dorset, D. L. The role of symmetry in building up zeolite frameworks from layered zeolite precursors having ferrierite and CAS layers. *Struct. Chem.* **2010**, *21*, 385.

(7) Xu, L.; Sun, J. Recent Advances in the Synthesis and Application of Two-Dimensional Zeolites. *Adv. Energy Mater.* **2016**, *6*, 1600441.

(8) Corma, A.; Fornes, V.; Pergher, S. B.; Maesen, T. L. M.; Buglass, J. G. Delaminated zeolite precursors as selective acidic catalysts. *Nature* **1998**, *396*, 353.

(9) Maheshwari, S.; Jordan, E.; Kumar, S.; Bates, F. S.; Penn, R. L.; Shantz, D. F.; Tsapatsis, M. Layer Structure Preservation during Swelling, Pillaring, and Exfoliation of a Zeolite Precursor. *J. Am. Chem. Soc.* **2008**, *130*, 1507.

(10) Sabnis, S.; Tanna, V. A.; Li, C.; Zhu, J.; Vattipalli, V.; Nonnenmann, S. S.; Sheng, G.; Lai, Z.; Winter, H. H.; Fan, W. Exfoliation of two-dimensional zeolites in liquid polybutadienes. *Chem. Commun.* **2017**, *53*, 7011.

(11) Gil, B.; Makowski, W.; Marszalek, B.; Roth, W. J.; Kubu, M.; Čejka, J.; Olejniczak, Z. High acidity unilamellar zeolite MCM-56 and its pillared and delaminated derivatives. *Dalton Trans* **2014**, *43*, 10501.

(12) Ogino, I.; Eilertsen, E. A.; Hwang, S.-J.; Rea, T.; Xie, D.; Ouyang, X.; Zones, S. I.; Katz, A. Heteroatom-Tolerant Delamination of Layered Zeolite Precursor Materials. *Chem. Mater.* **2013**, *25*, 1502.

(13) Corma, A.; Diaz, U.; Domine, M. E.; Fornés, V. AlITQ-6 and TiITQ-6: Synthesis, Characterization, and Catalytic Activity. *Angew. Chem., Int. Ed.* **2000**, *39*, 1499.

(14) Varoon, K.; Zhang, X.; Elyassi, B.; Brewer, D. D.; Gettel, M.; Kumar, S.; Lee, J. A.; Maheshwari, S.; Mittal, A.; Sung, C.-Y.; Cococcioni, M.; Francis, L. F.; McCormick, A. V.; Mkhoyan, K. A.; Tsapatsis, M. Dispersible Exfoliated Zeolite Nanosheets and Their Application as a Selective Membrane. *Science* **2011**, *334*, 72.

(15) Kosuge, K.; Tsunashima, A. New silica-pillared material prepared from the layered silicic acid of ilerite. New silica-pillared material prepared from the layered silicic acid of ilerite. *J. Chem. Soc., Chem. Commun.* **1995**, *23*, 2427.

(16) Roth, W. J.; Kresge, C. T.; Vartuli, J. C.; Leonowicz, M. E.; Fung, A. S.; McCullen, S. B. In *Studies in Surface Science and Catalysis*; Beyer, H. K., Karge, H. G., Kiricsi, I., Nagy, J. B., Eds.; Inorganic MCM-36: TEOS pillaring from swollen MCM(P); 1995; Vol. 94, p 301.

(17) Kresge, C. T.; Roth, W. J.; Simmons, K. G.; Vartuli, J. C. A method of preparing a pillared layered oxide material (Mobil Oil Corporation). WO Patent 92/011935, 1992.

(18) Kresge, C. T.; Roth, W. J.; Simmons, K. G.; Vartuli, J. C. Crystalline oxide material (Mobil Oil Corporation). U.S. Patent 5,229,341, 1993.

(19) Maheshwari, S.; Martínez, C.; Teresa Portilla, M.; Llopis, F. J.; Corma, A.; Tsapatsis, M. Influence of layer structure preservation on the catalytic properties of the pillared zeolite MCM-36. *J. Catal.* **2010**, *272*, 298.

(20) Jin, F.; Chang, C.-C.; Yang, C.-W.; Lee, J.-F.; Jang, L.-Y.; Cheng, S. New mesoporous titanosilicate MCM-36 material synthesized by pillaring layered ERB-1 precursor. *J. Mater. Chem. A* **2015**, *3*, 8715.

(21) Roth, W. J.; Gil, B.; Mayoral, A.; Grzybek, J.; Korzeniowska, A.; Kubu, M.; Makowski, W.; Čejka, J.; Olejniczak, Z.; Mazur, M. Pillaring of layered zeolite precursors with ferrierite topology leading to unusual molecular sieves on the micro/mesoporous border. *Dalton Trans* **2018**, *47*, 3029.

(22) Na, K.; Choi, M.; Park, W.; Sakamoto, Y.; Terasaki, O.; Ryoo, R. Pillared MFI Zeolite Nanosheets of a Single-Unit-Cell Thickness. *J. Am. Chem. Soc.* **2010**, *132*, 4169.

(23) Liu, B.; Wattanaprayoon, C.; Oh, S. C.; Emdadi, L.; Liu, D. Synthesis of Organic Pillared MFI Zeolite as Bifunctional Acid−Base Catalyst. *Chem. Mater.* **2015**, *27*, 1479.

(24) Emdadi, L.; Tran, D. T.; Zhang, J.; Wu, W.; Song, H.; Gan, Q.; Liu, D. Synthesis of titanosilicate pillared MFI zeolite as an efficient photocatalyst. *RSC Adv.* **2017**, *7*, 3249.

(25) Zhang, X.; Liu, D.; Xu, D.; Asahina, S.; Cychosz, K. A.; Agrawal, K. V.; Al Wahedi, Y.; Bhan, A.; Al Hashimi, S.; Terasaki, O.; Thommes, M.; Tsapatsis, M. Synthesis of Self-Pillared Zeolite Nanosheets by Repetitive Branching. *Science* **2012**, *336*, 1684.

(26) Agrawal, K. V.; Topuz, B.; Pham, T. C. T.; Nguyen, T. H.; Sauer, N.; Rangnekar, N.; Zhang, H.; Narasimharao, K.; Basahel, S. N.; Francis, L. F.; Macosko, C. W.; Al-Thabaiti, S.; Tsapatsis, M.; Yoon, K. B. *Adv. Mater.* **2015**, *27*, 3243.

(27) Zou, C.; Lin, L. C. Exploring the potential and design of zeolite nanosheets as pervaporation membranes for ethanol extraction. *Chem. Commun.* **2018**, *54*, 13200.

(28) Zhang, H.; Xiao, Q.; Guo, X.; Li, N.; Kumar, P.; Rangnekar, N.; Jeon, M. Y.; Al-Thabaiti, S.; Narasimharao, K.; Basahel, S. N.; Topuz, B.; Onorato, F. J.; Macosko, C. W.; Mkhoyan, K. A.; Tsapatsis, M. Open-Pore Two-Dimensional MFI Zeolite Nanosheets for the Fabrication of Hydrocarbon-Isomer-Selective Membranes on Porous Polymer Supports. *Angew. Chem., Int. Ed.* **2016**, *55*, 7184.

(29) Meng, L.; Zhu, X.; Hensen, E. J. M. Stable Fe/ZSM-5 Nanosheet Zeolite Catalysts for the Oxidation of Benzene to Phenol. *ACS Catal.* **2017**, *7*, 2709.

(30) Jung, J.; Jo, C.; Cho, K.; Ryoo, R. Zeolite nanosheet of a single-pore thickness generated by a zeolite-structure-directing surfactant. *J. Mater. Chem.* **2012**, *22*, 4637.

(31) Choi, M.; Na, K.; Kim, J.; Sakamoto, Y.; Terasaki, O.; Ryoo, R. Stable single-unit-cell nanosheets of zeolite MFI as active and long-lived catalysts. *Nature* **2009**, *461*, 246.

(32) Fan, W.; Snyder, M. A.; Kumar, S.; Lee, P.-S.; Yoo, W. C.; McCormick, A. V.; Lee Penn, R.; Stein, A.; Tsapatsis, M. Hierarchical nanofabrication of microporous crystals with ordered mesoporosity. *Nat. Mater.* **2008**, *7*, 984.

(33) Chen, H.; Wydra, J.; Zhang, X.; Lee, P.-S.; Wang, Z.; Fan, W.; Tsapatsis, M. Hydrothermal Synthesis of Zeolites with Three-Dimensionally Ordered Mesoporous-Imprinted Structure. *J. Am. Chem. Soc.* **2011**, *133*, 12390.

(34) Liu, D.; Bhan, A.; Tsapatsis, M.; Al Hashimi, S. Catalytic Behavior of Brønsted Acid Sites in MWW and MFI Zeolites with Dual Meso- and Microporosity. *ACS Catal.* **2011**, *1*, 7.

(35) Innocenzi, P. *The Sol to Gel Transition*; Springer Briefs in Materials, Springer International Publishing: 2016; p 7.

(36) Busca, G. pectroscopic characterization of the acid properties of metal oxide catalysts. *Catal. Today* **1998**, *41*, 191.

(37) Jiang, M.; Karge, H. G. *J. Chem. Soc., Faraday Trans.* **1996**, *92*, 2641.

(38) Trombetta, M.; Busca, G. On the Characterization of the External Acid Sites of Ferrierite and Other Zeolites: A Reply to Pieterse et al. *J. Catal.* **1999**, *187*, 521.

(39) Bai, Y.; Wei, L.; Yang, M.; Chen, H.; Holdren, S.; Zhu, G.; Tran, D. T.; Yao, C.; Sun, R.; Pan, Y.; Liu, D. Three-step cascade over a single catalyst: synthesis of 5-(ethoxymethyl)furfural from glucose over a hierarchical lamellar multi-functional zeolite catalyst. *J. Mater. Chem. A* **2018**, *6*, 7693.

(40) Kolodziejski, W.; Zicovich-Wilson, C.; Corell, C.; Perez-Pariente, J.; Corma, A. 27Al and 29Si MAS NMR Study of Zeolite MCM-22. *J. Phys. Chem.* **1995**, *99*, 7002.

(41) Camblor, M. A.; Corma, A.; Díaz-Cabañas, M.-J.; Baerlocher, C. Synthesis and Structural Characterization of MWW Type Zeolite ITQ-1, the Pure Silica Analog of MCM-22 and SSZ-25. *J. Phys. Chem. B* **1998**, *102*, 44.

(42) Xu, D.; Abdelrahman, O.; Ahn, S. H.; Guefrachi, Y.; Kuznetsov, A.; Ren, L.; Hwang, S.; Khaleel, M.; Al Hassan, S.; Liu, D.; Hong, S. B.; Dauenhauer, P.; Tsapatsis, M. A quantitative study of the structure–activity relationship in hierarchical zeolites using liquid-phase reactions. *AIChE J.* **2019**, *65*, 1067.

(43) Liu, D.; Zhang, X.; Bhan, A.; Tsapatsis, M. Activity and selectivity differences of external Brønsted acid sites of single-unit-cell thick and conventional MFI and MWW zeolites. *Microporous Mesoporous Mater.* **2014**, *200*, 287.

(44) Emdadi, L.; Oh, S. C.; Wu, Y.; Oliaee, S. N.; Diao, Y.; Zhu, G.; Liu, D. The role of external acidity of meso-/microporous zeolites in determining selectivity for acid-catalyzed reactions of benzyl alcohol. *J. Catal.* **2016**, *335*, 165.